Published in final edited form as:
J Colloid Interface Sci. 1996 March 25; 178(2): 775–784. doi:10.1006/jcis.1996.0177.

An AFM Study of the Effects of Silanization Temperature, Hydration, and Annealing on the Nucleation and Aggregation of Condensed OTS Domains on Mica

David W. Britt and **Vladimir Hlady**
Department of Bioengineering, University of Utah, Salt Lake City, Utah 84112

Abstract

Partial monolayers of octadecyltrichlorosilane (OTS) were formed on mica under different reaction conditions in which the silanization temperature, time, and amount of water adsorbed on the mica substrates were varied. OTS surface coverage increased with silanization time for all samples; however, the amount and distribution of adsorbed OTS varied greatly under these different reaction conditions. AFM analysis showed that OTS formed two phases on mica silanized at 25°C: condensed “island-like” domains and expanded “liquid-like” domains. Partially dehydrated mica silanized at 9°C, however, displayed only condensed domains which were of smaller size compared to those on the 25°C samples. The lateral diffusion and aggregation of small condensed OTS domains to form larger aggregates was evident on all surfaces except the 25°C partially dehydrated mica. A uniform distribution of many small condensed domains surrounded by expanded OTS phases was seen instead. Extended annealing resulted in surface diffusion and aggregation of these domains and nucleation of new condensed domains from the surrounding expanded OTS phases. These observations are consistent with a deposition, diffusion, and aggregation model (DDA) which allows for activated diffusion; however, rigorous modeling is not presented here.

Keywords

atomic force microscope; self-assembled monolayer; submonolayer; octadecyltrichlorosilane

INTRODUCTION

Self-assembled monolayers (SAMs) have many potential applications in a wide variety of fields and their ease of preparation and durability make SAMs an appealing alternative to Langmuir–Blodgett monolayers (1, 2). The surface chemistry of many materials, such as gold, alumina, mica and oxidized silicon can be modified using SAMs. Hydrophilic surfaces such as cleaved mica can be made hydrophobic through the self-assembly of molecules with hydrophobic “tail groups” such as octadecyltrichlorosilane (OTS). Similarly, SAMs with chemically reactive tail groups can be formed and further chemically modified, thus

Correspondence to: Vladimir Hlady.

allowing for the formation of multilayers (2). To the contrary, incomplete, submonolayers can be formed by quenching the self-assembly process before it reaches completion (3).

Under submonolayer conditions the surface is often described as either being uniformly covered with an expanded monolayer of decreased height or intermittently covered with condensed “islands” of monolayer (2–6). Thus a microheterogeneous surface of mixed surface chemistry can be created. SAMs can also be used to construct a “macro”-heterogeneous surface in which one end of a silica plate is made hydrophobic while the other is left hydrophilic and the intervening regions display intermediate character (7). These hydrophobicity gradient surfaces are useful in the study of protein adsorption phenomena since an adsorbing protein encounters a surface of varying surface energy. Peculiar adsorption behavior has been noted for certain proteins in the transition regions of the gradient surfaces using total internal reflection fluorimetry (TIRF), and it is believed that the amphipathic nature of certain proteins is satisfied upon adsorbing to the gradient regions (8).

These findings have motivated us to investigate protein adsorption on surfaces with microheterogeneities using a high resolution technique such as atomic force microscopy (also referred to as scanning force microscopy, SFM) (9). The atomic force microscope is capable of nanometer resolution and is often used to study proteins on surfaces (10–13). However, the surfaces used in AFM studies have generally been homogenous in terms of surface chemistry, either being fully wetting or completely hydrophobic. The formation of partial SAMs which display discrete monolayer “islands” provides a method for creating microheterogeneous surfaces with hydrophobic and hydrophilic domains with dimensions on the order of several protein diameters. Furthermore, these partial monolayers could potentially be “back-filled” with a second type of self-assembling molecule, creating a complete mixed monolayer composed of distinct domains (14). Although self-assembly of a binary mixture of two SAM types would be more convenient and logical, segregation of the two SAM types into domains larger than 50 nm does not occur (15, 16). Langmuir–Blodgett transferred films are better suited for their macroscopic phase separation in mixed monolayers (17, 18).

The main parameters governing submonolayer formation are the flux, or deposition, of the monomers (and any pre-polymerized oligomers in the bulk) to the surface and the lateral diffusion, and possible aggregation, of these species once they reach the surface. To describe our results we will use the following terminology: A *monomer* refers to a single OTS molecule. A *cluster* is a condensed assembly of monomers — in the context of this paper, a cluster will be an oligomer which is clearly resolved by the AFM probe (~50–100 nm diameter). An *island* is simply an aggregate of clusters and monomers. A *condensed domain* refers to an island or cluster, and an *expanded phase* refers to disordered monomers and oligomers which have not self-assembled to form condensed domains.

The ratio of the flux to the diffusion coefficient gives the normalized flux which dictates the size, morphology and surface distribution of clusters as described in the deposition, diffusion, and aggregation model (DDA) of Stanley and co-workers (19–21). In the absence of long ranged lateral forces a monomer, oligomer, or cluster diffusing on the surface executes a random walk and eventually encounters another monomer, oligomer, or cluster

on the surface. Monomer–monomer encounters result in the nucleation of clusters and monomer–cluster and cluster–cluster encounters result in the propagation (self-assembly) of larger clusters (islands) on the surface. Aggregation is generally assumed to be irreversible due to the nonequilibrium kinetics of submonolayer formation (16). The shape of OTS islands assembled on mica can be fractal-like, suggesting that activated diffusion and rearrangement of clusters is absent or very minimal. However, the temporal arrangement of islands and other surface domains is a nonequilibrium morphology and surface rearrangements are expected to eventually occur. Increasing the temperature of the system (either during or after the silanization process) drives the system toward equilibrium and is manifested by the presence of fewer, more compact clusters. This behavior is fully accounted for in models of DDA which include activated diffusion (22, 23). The effects of activated diffusion were observed in the partial OTS monolayers created here by varying the silanization temperature and through postsilanization annealing. Thus, it is possible to control the morphology of submonolayers, forming surfaces with either a few discrete islands composed of many clusters or surfaces with many discrete small clusters. Under certain conditions such as low temperatures, the cluster sizes would be so small that a “uniform” growth mechanism could be used to describe the monolayer growth. Similarly, at high temperatures only a disordered expanded phase may be present and again a uniform growth mechanism may be used to model monolayer growth. These concepts are discussed below.

Both island (24, 25) and uniform growth mechanisms (4, 6) have been reported for OTS assembly on silica substrates; thus the properties of the substrate alone do not dictate which model prevails. Parameters such as silanization temperature and hydration greatly influence monolayer self-assembly (26–31). A solvent independent critical temperature of around 28°C for OTS monolayer formation on silica has been identified; above this temperature adsorbed OTS molecules are disordered and expanded and below which they are closely packed and ordered (29–31). Similarly, the amount of water present in the reaction solution and at the solution–substrate interface also influences the packing and organization of the monolayer. Tripp and Hair have demonstrated that OTS monolayers do not form on completely dehydrated silica (26, 27) and Carson and Granick report similar results for dehydrated mica (28). The self-assembly process requires a certain amount of water (either in the bulk solution or on the substrate surface) to hydrolyze the OTS molecules. In addition, interfacial water acts as a lubricating layer on which adsorbed molecules laterally diffuse and aggregate (29, 31). Barrat *et al.* introduced water in the silanization solution and exposed their silica substrates to water saturated nitrogen to produce OTS monolayers composed of many self-similar domains (24). Similarly, Schwartz *et al.* exposed their mica substrates to steam prior to silanization (3). Angst and Simmons report that hydrated silica surfaces produce close-packed OTS monolayers while dry surfaces have diminished monolayer coverage (4). Likewise, Wasserman *et al.* report that the formation of complete monolayers in a dry nitrogen atmosphere takes 10 times longer than monolayers formed in the ambient laboratory environment (6). In terms of the DDA model, the presence of a hydration layer increases the surface diffusivity of the adsorbing species, leading to a decreased normalized flux which results in the formation of fewer, but larger, islands.

Conversely, OTS molecules adsorbing on a dehydrated surface have a decreased surface diffusivity which is manifested by the formation of many small clusters.

Controlling hydration and temperature during silanization is important if reproducible SAMs are to be created (29). Our attempts to form reproducible, stable, submonolayers of OTS on mica support this. The presence of expanded OTS phases (i.e., disordered OTS monomers and oligomers) in addition to the condensed OTS clusters and islands has complicated our attempts to create model surfaces for protein adsorption. In addition, partial monolayers of OTS on mica were often unstable in aqueous solutions — possibly a result of too thick a water layer in between the monolayer and the mica or a manifestation of the chemical unreactivity of cleaved mica. In this paper, we report the effects of silanization temperature, substrate hydration, and silanization time on the formation of partial monolayers of OTS on mica; the ratio of expanded OTS phases to condensed OTS clusters and islands and the size and distribution of the latter depend on these variables. In addition, postsilanization annealing of OTS monolayers on mica is shown to enhance surface diffusion and aggregation of adsorbed OTS species, leading to an expanded phase to condensed phase transition. These observations are consistent with a DDA model of submonolayer formation which allows for activated diffusion.

MATERIALS AND METHODS

Modifications of the silanization procedure given by Schwartz *et al.* were used to create partial OTS monolayers on mica (3). Two silanization temperatures (25 and 9°C) and two surface hydration states were employed during silanization. Figure 1 is a general outline of how the mica surfaces were prepared.

Preparation of OTS on Partially Dehydrated Mica Surfaces (25°C)

All reaction vessels were cleaned in a 70°C chromo-sulfuric acid bath (Chromerge Monostat) for at least 6 h followed by extensive rinsing with 0.2 μm filtered deionized water, then dried in a desiccator oven. Dicyclohexyl (Aldrich) was passed through a column of basic alumina (ICN Biomedical) prior to use. OTS (Hüls) and chloroform (EM Science) were used as received. A 0.5 *M* HCl solution was prepared using double-distilled water. The mica samples (Ashville Shoonmaker) were cleaved with adhesive tape and handled with acid cleaned stainless steel tweezers.

All reactions were carried out in a fume hood under ambient conditions (25°C, 20% relative humidity, RH). Mica disks (1 cm in diameter and 1 mm thick) were cleaved on both faces then placed in a 0.5 *M* HCl solution for 2 h. The mica disks were withdrawn from the acid solution and excess liquid was removed under a gentle stream of nitrogen filtered through a 0.2 μm filter (Millipore). The disks were then placed in a nitrogen oven at 115°C for 20 min, then allowed to cool to room temperature in a covered glass petri dish. While the mica was cooling, a 0.5 m*M* solution of OTS in dicyclohexyl was prepared. The mica disks were individually immersed in the OTS solution for times ranging from 10 s to 5 min, then removed and immediately placed in a stirred chloroform bath for 2 min. The samples were then removed and dried under a stream of 0.2 μm filtered nitrogen.

Preparation of OTS on Partially Dehydrated Mica Surfaces (9°C)

This procedure was identical to the 25°C procedure except that the OTS solution was cooled to 9°C using a 25 ml reaction vessel with an integral water jacket. The OTS solution was prepared in the reaction vessel and a steady flow of 9°C water was circulated through the jacket to cool the OTS solution. Once the solution temperature was 9°C, the oven-dried mica disks were silanized as described above.

Preparation of OTS on Hydrated Mica Surfaces

The mica disks were cleaved on both sides then placed in a jet of steam for about 30 s a side. Water condensate on the samples was removed with a gentle stream of nitrogen before silanizing the samples. Silanization was carried out in a freshly prepared 0.5 m*M* OTS solution (25°C) in dicyclohexyl for times ranging from 10 s to 5 min. The silanized samples were removed and immediately placed in a stirred chloroform bath for 2 min, then removed and dried under a stream of 0.2 μm filtered nitrogen.

Characterization of Surfaces

Silanized samples were analyzed with sessile drop contact angle under ambient conditions using a goniometer (Ramé-Hart, A-100). Several 3–5 μl drops of double distilled water were placed near the perimeters of the samples and their average values reported as receding water contact angles. The contact angles of drops which were allowed to remain on the surfaces for 15 min did not change during this time. Samples were also analyzed with contact mode atomic force microscopy (AFM) using a Digital Instruments Nanoscope II AFM. Scanning was done at 25°C in both air and aqueous environments (images of the latter are not presented here). The feedback or “height” mode of operation was employed and Park Scientific cantilevers (nominal spring constant ~0.05 N/m and tip radius of curvature ~20 nm) were used. Different areas on each sample were compared to verify that the areas being analyzed were typical of the overall surface topography. Areas where contact angle measurements were made were not scanned since the water drops can potentially alter the monolayer. Analysis and presentation of the AFM data was done using NIH Image 1.55.

Extended Annealing of the OTS Modified Surfaces

Postsilanization annealing of the OTS samples prepared on the 25°C partially dehydrated mica was done at 115°C in an oven purged with 0.2 μm filtered nitrogen. Samples were aged for a total of 42.5 h; however, this process was interrupted after 1.5,4.75, and 19.75 h so that the effects of the annealing process could be monitored with time. After AFM and contact angle measurements were made, the samples were immediately returned to the nitrogen oven for further annealing.

RESULTS

Figure 2 shows a typical set of AFM images of OTS monolayers assembled on mica at different silanization temperatures and degrees of surface hydration; these surfaces have not been annealed and were imaged within 48 h after preparation. The bright features in these images are condensed OTS domains (clusters and islands) and the darker features in the background are expanded OTS phases and the mica surface. The condensed domains are

between 2.4 and 2.6 nm high (measured relative to the mica background) which is consistent with a single OTS monolayer (2). The receding water contact angles measured on these surfaces are given in the lower left corners of the images. The increase in water contact angle at longer silanization times indicates that the OTS molecules adsorbed with their polar head groups on the mica surface and their hydrophobic tail groups exposed to the solution.

OTS Assembly on Hydrated Mica (25°C)

The surfaces shown in Figs. 2a–2c were silanized at 25°C on hydrated mica for 10, 40, and 300 s, respectively. Expanded OTS phases (light gray features) are discernible in between the condensed OTS clusters and islands (bright features) in Fig. 2a. The dark background is the mica surface. The average island diameter in Fig. 2a is about 200 nm. Small OTS clusters (~50 nm diameters) are also present. In Fig. 2b, the expanded phase is less prevalent and the island diameters have increased to an average of about 1 μm. In Fig. 2c, the surface is almost completely covered with OTS except at the interisland junctions where many small “pinholes” exist.

OTS Assembly on Partially Dehydrated Mica (25°C)

Figures 2d–2f show three surfaces also silanized at 25°C, but on partially dehydrated mica. A uniform distribution of OTS clusters (bright features) on the surfaces is seen in all three images, however, no large islands are present. This suggests that the surface diffusivity of the OTS species on partially dehydrated mica is less than on hydrated mica. The average cluster diameters are about 50, 100, and 180 nm respectively. Expanded OTS phases (light gray areas) are still discernible in between the condensed domains on the partially dehydrated mica surfaces.

OTS Assembly on Partially Dehydrated Mica (9°C)

Figures 2g–2i and Fig. 3 show partially dehydrated mica surfaces silanized at 9°C and observed at room temperature. After 10 s of silanization (Fig. 2g) many small (~50 nm average diameter) condensed domains are noted. After 40 s of silanization (Fig. 2h) larger aggregates of condensed OTS are clearly seen, however, many smaller condensed domains (~60 nm average diameter) are also present. After 300 s of silanization (Fig. 2i) the aggregates of condensed OTS are even larger, forming well defined islands. Smaller condensed domains (~80 nm diameter) are still present. Figure 3 shows a depletion of the condensed domains around the perimeter of “growing” islands. Little or no expanded OTS phases are seen on these surfaces prepared at 9°C.

Annealing the 25°C Partially Dehydrated Mica

The samples shown in Figs. 2d–2f were annealed for 42.5 h at 115°C and the results are shown in Figs. 4 and 5. Figure 4 shows the 10 s sample of Fig. 2d after 42.5 h of annealing at 115°C. This sample was also analyzed after 4.75 and 19.75 h; however, no significant changes in the surface were noted with the AFM. After annealing for 42.5 h, however, the number of clusters on this surface was seen to increase three-fold. Average cluster diameters also increased from about 50 to about 100 nm and the background displayed a more uniform appearance following annealing. No cluster aggregation was evident for this sample though.

The water contact angle for this sample remained constant throughout annealing at 40° ± 3°, indicating no net loss or reorientation of OTS from the surface during annealing.

Figures 5a–5d show the 300 s sample (Fig. 2f) after 1.5, 4.75, 19.75, and 42.5 h of annealing at 115°C, respectively. It is clear that the clusters aggregated during annealing, forming large islands of OTS (as shown in Fig. 5e). It was noted that some smaller clusters appeared after 4.75 h of annealing which were not present after 1.5 h of annealing. These clusters may have nucleated from expanded OTS during this short annealing time; however, the sample silanized for 10 s (Fig. 2d) did not show any increase in the number of clusters after only 4.75 h of annealing (data not shown). It is likely that these clusters were present after 1.5 h of annealing but were effectively “hidden” from the AFM probe due to a close packing arrangement — that is, two small clusters in close proximity would appear as one larger cluster to a relatively blunt AFM probe. Annealing may have isolated some small clusters from neighboring clusters during the early stages, while at later stages it appears that the smaller clusters have irreversibly aggregated to form the larger islands.

The sample contact angle remained relatively constant at 95° ± 5° throughout the annealing process, again indicating no net loss of molecules from the surface during annealing. The 40 s sample (Fig. 2e) displayed similar behavior upon annealing (data not shown).

DISCUSSION

AFM Tip Effects

The size of the features shown in the AFM images here are not true representations due to broadening and convolution effects of the AFM probe. The cluster and island dimensions reported in this paper are the uncorrected values. Assuming a spherical probe of 20 nm radius it is possible to correct for broadening effects using the chord theorem (32). The smallest OTS clusters resolved in the images shown here measured about 50 nm in diameter and, when broadening is corrected for, the size of these clusters may actually be closer to 30 nm in diameter. A circular cluster this size will contain about 3500 OTS monomers, assuming that each OTS monomer in a cluster is close packed and has a footprint of about 0.2 nm^2 (2).

The vertical resolution of the AFM probe indicates that the expanded OTS phases are about 1 to 2 nm shorter than the condensed OTS phases. Whether this height difference is true or whether it is a result of the AFM probe compressing the loosely packed expanded OTS molecules is not known. The expanded OTS is expected to be more compliant than the condensed OTS which will result in a convolution of OTS topography with sample compliance. However, given the low packing arrangement and greater conformational freedom of expanded OTS, a decreased height is not surprising. In addition, applied forces were kept at a minimum during scanning to avoid excess sample manipulation by the probe. The condensed OTS monolayer heights reported here agree with values attained using spectroscopic methods (2) and can be considered reliable.

OTS Self-Assembly on Mica

OTS condensed domain growth occurs by surface diffusion and aggregation of adsorbed OTS monomers/oligomers and by continued deposition of OTS monomers and prepolymerized oligomers from the bulk solution (2, 3). The *in situ* surface diffusion of OTS condensed domains to form larger aggregates is indicated by the self-similar, repetitive morphologies of the OTS islands shown in Fig. 2. The effect of temperature and surface hydration on cluster size, shape and distribution is also seen in Fig. 2. The pinholes seen in Fig. 2c and in Fig. 2i are defects which form at cluster–cluster interfaces due to an imperfect packing and monolayer reorganization process. The distribution of clusters is homogeneous across the surfaces as shown in Fig. 2; however, the aggregation of clusters to form larger islands appears to only occur at certain nucleation sites as seen in Fig. 2h and Fig. 3. The continued existence of many small clusters among these larger islands supports a heterogeneous island nucleation theory. Bierbaum and Grunze report a similar distribution of OTS clusters and islands on silicon substrates (25). It is not known why cluster aggregation occurs more readily at certain sites on the mica surface, this may be a result of an uneven distribution of water on the surface during silanization or other local changes of the mica surfaces such as counterion density. Perhaps the HCl pretreatment has increased the number of cluster nucleation sites on the surface.

Expanded OTS Phases

Contact angle analysis and AFM images (Figs. 2a and 2d) support the presence of disordered, expanded phases of OTS on mica surfaces silanized at 25°C. The height of the expanded phase was usually between 0.5 and 2 nm. The nucleation of condensed OTS domains from expanded OTS phases was demonstrated through extended annealing (42.5 h at 115°C) of a partially dehydrated sample which was silanized at 25°C for 10 s (Figs. 2d and 4). Why the expanded phase is so prevalent on the hydrated mica sample silanized at 25°C (Fig. 2a) is not well understood. We believe that this may be explained thermodynamically in terms of the increase in entropy as discussed below.

Effect of Hydration on Monolayer Formation

The amount of water present on the mica during silanization is largely unknown. One expects, however, that the oven-treated mica will have less water on its surface than the steam treated mica. We believe that some water was present on the mica after the oven treatment since OTS did self-assemble on these surfaces — cleaved mica surfaces which were dried overnight in a vacuum oven (25 in Hg below ambient pressure, 70°C) prior to silanization under ambient conditions did not form monolayers. Assuming that the reduced atmosphere, 70°C samples contained less surface water than the 115°C samples, then these results support the findings of others that a certain amount of water is required for monolayer self-assembly. In addition to any differences in surface hydration, the reduced atmosphere, 70°C samples were never exposed to steam or treated with HCl, procedures which are designed to enhance self-assembly. Another factor which may also have influenced OTS self-assembly on the reduced atmosphere, 70°C samples was the large delay between cleavage of the mica and OTS modification. Bierbaum and Grunze demonstrate that different preparation environments affect the OTS assembly process on silicon (25). The

role of surface water as a “lubricating” layer on which OTS molecules diffuse is evident in comparing the hydrated surfaces with the partially dehydrated surfaces in Fig. 2. The condensed domain sizes in the images in the first column in Fig. 2 are significantly larger than those in the second column of Fig. 2. The presence of a water layer between the OTS and the mica substrate may explain the decreased stability of OTS in aqueous solutions. A thick water layer may diminish the non-covalent interactions between the polar head group of OTS and the surface as well as prevent covalent bond formation between OTS molecules and any surface hydroxyl groups.

The dicyclohexyl solvent used for silanizing the surfaces was passed through a column of basic alumina to remove the trace amounts of water. This step was done to deter pre-polymerization of the OTS before the mica samples were inserted. An additional precaution would be to handle all solutions in a glove box purged with dry nitrogen — however, the humidity in our labs is, as a rule, very low (less than 20% RH) and this precaution was not heeded. With regards to cooling the OTS solution to 9°C, the water flowing through the vessel jacket was completely isolated from the OTS solution and did not directly introduce any water to the solution. However, the condensation of ambient water on the cooled vessel may be a problem in humid labs. A more elegant cooled reaction vessel is described by Brzoska *et al.* (29).

Effects of Silanization Temperature and Annealing on Monolayers

The samples silanized at 9°C displayed distinct surface morphologies. The most obvious effect of temperature is on cluster size: compare Fig. 2a with Fig. 2g. Both samples were silanized for 10 s; however, the 9°C sample has many small clusters while the 25°C sample has few, large clusters. This finding suggests that the normalized flux for the 9°C sample is larger than that for the 25°C sample. The enhanced cluster growth with temperature is largely a kinetic effect which demonstrate how cluster growth and nucleation are competing processes. A similar dependence of cluster size on temperature is seen for the epitaxial growth of Fe on Fe(001) (33). However, the expanded OTS phase is also more prevalent at 25 than at 9°C. This is most likely a thermodynamic effect. The many small OTS clusters (≤ 100 nm diameters) present in Figs. 2g–2i indicate that these domains grow slowly with silanization time. The coexistence of these small clusters in the presence of large islands suggests that cluster aggregation only occurs at a few select sites on the surface. Whether these sites are determined by the substrate, the clusters, or both is not known. Figure 3 shows how aggregation of clusters to form a larger island, composed of multiple clusters, results in the depletion of clusters around the perimeter of the island. This suggests that the growing island acts like a “sink” for clusters (and possibly monomers). This localized depletion was not seen around all of the islands, however, as observed in Figs. 2h and 2i.

Another distinction between the 9°C samples and the 25°C samples is the shape of the islands; the 9°C islands have more dendritic processes than those prepared at 25°C. The latter are much more compact while the former are more fractal-like. This is consistent with an activated diffusion process in which particles situated at the perimeters of the clusters rearrange at “elevated” temperatures (25°C) to form more compact structures while at lower temperatures (9°C) the edge particles remain fractal-like (21, 22, 34).

Post-silanization annealing of the OTS monolayers had three noticeable effects: an increase in the number of clusters, a decrease in the amount of expanded OTS and the aggregation of clusters to form larger islands (see Figs. 4 and 5). No significant change in sample contact angles occurred during annealing, indicating that the relative amount and net amphiphilic orientation of OTS molecules on the surfaces remained constant. Cohen *et al.* report that covalently bound OTS monolayers are stable to annealing up to temperatures of 140°C (35). Whether OTS is covalently bound to the mica substrates used here is uncertain. The increase in the number of clusters after 42.5 h of annealing shown in Fig. 4 suggests that clusters were nucleated from existing expanded phases. No aggregation of the clusters was evident. Cluster aggregation resulting from annealing is evident at higher surface coverages as seen in Fig. 5. The ability of the clusters to aggregate, forming larger islands of OTS for the 300 s sample and not for the 10 s sample is a manifestation of the overall low diffusivity of OTS on mica in air at 115°C. Stranick *et al.* demonstrate nanometer sized rearrangements of monolayer at room temperature using STM (16). The cluster domains on the 300 s sample were in closer proximity prior to annealing and did not have to diffuse more than 50 to 100 nm before encountering another condensed domain. In addition, cluster nucleation from expanded phases may have occurred which would not be evident in the images in Fig. 5 due to the high surface coverage of clusters and limited AFM probe resolution.

The nucleation of clusters from expanded phases and the aggregation of existing clusters during postsilanization annealing appears to be largely under kinetic control. Thus, an increase in temperature provides the thermal energy for OTS surface diffusion. Once diffusing OTS monomers/oligomers encounter each other, favorable hydrophobic interactions among the tail groups are probably responsible for their aggregation. It is not known whether any covalent linkages are formed upon aggregation during postsilanization annealing. The presence of expanded OTS phases and the formation of condensed OTS clusters and islands *in situ* appears to be governed by both kinetics and thermodynamics. Whitesides *et al.* gives a brief thermodynamic treatment of monolayer self-assembly (36). A decrease in the silanization solution temperature leads to a decrease in the entropic energy contribution ($T\Delta S$) and favors the formation of ordered, condensed clusters. The kinetics of *in situ* domain formation are also decreased at lower temperatures which is manifested by the smaller size of clusters and the fractal nature of cluster aggregates seen in the 9°C samples. The clusters and islands formed at 25°C are larger than those formed at 9°C due to the increased diffusivity and the expanded OTS phase is more prevalent at 25°C due to an increase in entropy. The nature and organization of the expanded phase is not clear; however, it is expected that some hydrophobic interactions are present among the OTS tail groups. This would explain why the expanded OTS phase was not observed for the 9°C samples since a decrease in hydrophobic interactions is expected with decreasing temperature. This would also explain why the cluster sizes are much smaller for surfaces silanized at 9°C.

Mica HCl Pretreatment

The effects of HCl treatment on the binding of OTS to the mica surface are unknown. The HCl treatment is designed to produce surface hydroxyl groups on mica, similar to the steam treatment procedure (3, 28). Pashley has demonstrated that mica surfaces exposed to slightly

acidic solutions (pH ~ 6) undergo complete exchange of K^+ counterions for solution H^+ ions (37). He also observed that the magnitude of the repulsive hydration force depended on the counterion nature and its concentration in solution. The exchange of counterions during the HCl pretreatments may have had an effect on OTS self-assembly; however, it is not possible to directly compare any counterion-hydration effects on OTS self-assembly since the amount of water introduced on the surfaces was intentionally different. However, any changes in silicate ion surface chemistry are probably subtle when compared to the effects of directly hydrating the mica surfaces. Furthermore, heating the HCl-treated mica at 115°C for 20 min may have condensed adjacent hydroxyl groups on the surface.

Controlling the amount of water on surfaces prior to silanization is important if reproducible monolayers are to be formed. Removing excess surface water in a nitrogen oven prior to silanization is only a qualitative method of controlling the hydration state of the surface. Granick *et al.* used a more controlled method to hydrate mica by placing the mica in a reduced atmosphere into which water vapor was introduced prior to OTS silanization (28). Barrat *et al.*, to the contrary, introduced a controlled water content into the solvent (24).

Monolayer Stability

Compared to complete monolayers, partial monolayers are much less stable due to the absence of lateral interactions at the edges of condensed domains. AFM analysis under aqueous solution of the partial monolayers prepared on hydrated mica at 25°C showed that the condensed domains were loosely bound to the surface and could be easily removed after several scans with the AFM probe. Furthermore, rearrangement of expanded phases in solution was also noted (results not shown here). Partially dehydrated mica silanized at 9°C produced partial monolayers which appeared to be composed of only condensed domains. These surfaces proved much more stable under aqueous solution, including a 0.01 *M* phosphate buffered saline solution. Preliminary *in situ* protein adsorption experiments using human low density lipoprotein on these surfaces were encouraging. Back-filling these surfaces with a second type of self-assembling molecule has not yet been tried. Although Mathauer and Frank report that their binary monolayers prepared in this manner are a random mixture of the two components, it is unlikely that their partial monolayers contained sizable (>100 nm) condensed domains to begin with (14).

CONCLUSIONS

The diffusion and aggregation of OTS adsorbed on mica substrates to form condensed clusters and islands has been shown. OTS surface diffusivity appears to be greater on hydrated surfaces than on dehydrated surfaces, further implicating the role of surface water as a lubricating layer between the monolayer and the substrate. The presence of expanded OTS phases in addition to the condensed clusters was noted for the samples prepared at 25°C, but not for samples prepared at 9°C. These latter samples displayed only condensed OTS clusters of smaller lateral dimensions compared to those on surfaces silanized at 25°C. Postsilanization annealing showed that OTS monolayers are still diffusive and allows for further modification of the monolayer. The stability of these monolayers under aqueous solution and their usefulness as model surfaces for protein adsorption is under investigation.

Acknowledgments

This work was financially supported by NIH Grant HL 44538 and the NIH Training Grant Fellowship awarded to David Britt.

References

1. Swalen JD, Allara DL, Andrade JD, Chandross EA, Garoff S, Israelachvili J, McCarthy TJ, Murray R, Pease RF, Rabolt JF, Wynne KJ, Yu H. Langmuir. 1986; 3:932.
2. Ulman, A. An Introduction to Ultrathin Organic Films. Academic Press; San Diego: 1991.
3. Schwartz DK, Steinberg S, Israelachvili J, Zasadzinski JAN. Phys Rev Lett. 1992; 69:3354. [PubMed: 10046797]
4. Angst DL, Simmons GW. Langmuir. 1991; 7:2236.
5. Tidswell IM, Rabedeau TA, Pershan PS, Kosowsky SD, Folkers JP, Whitesides GM. J Chem Phys. 1991; 95:2854.
6. Wasserman SR, Whitesides GM, Tidswell IM, Ocko BM, Pershan PS, Axe JD. J Am Chem Soc. 1989; 111:5852.
7. Lin YS, Hlady V. Colloids Surf B. 1994; 2:481.
8. Gölander CG, Lin YS, Hlady V, Andrade JD. Colloids Surf. 1990; 49:289.
9. Ho C-H, Britt DW, Hlady V. J Mot Recog. in press.
10. Siedlecki CA, Eppell SJ, Marchant RE. J Biomed, Mater Res. 1994; 28:971. [PubMed: 7814438]
11. Lea AS, Pungor A, Hlady V, Andrade J, Herron JN, Voss EW Jr. Langmuir. 1992; 8:68.
12. Hansma HG, Hoh JH. Annu Rev Biophys Biomol Struct. 1994; 23:115. [PubMed: 7919779]
13. Margel S, Vogler EA, Firment L, Watt T, Haynie S, Sogah DY. J Biomed Mater Res. 1993; 27:1463. [PubMed: 8113233]
14. Mathauer K, Frank CW. Langmuir. 1993; 9:3446.
15. Bain CD, Evall J, Whitesides GM. J Am Chem Soc. 1989; 111:7155.
16. Stranick SJ, Parikh AN, Tao Y-T, Allara DL, Weiss PS. J Phys Chem. 1994; 98:7636.
17. Chi LF, Fuchs H, Johnston RR, Ringsdorf H. Thin Solid Films. 1994; 242:151.
18. Ge S, Takahara A, Kajiyama T. Langmuir. 1995; 11:1341.
19. Jensen P, Barabási AL, Larralde H, Havlin S, Stanley HE. Phys Rev E. 1994; 50:618.
20. Jensen P, Barabási AL, Larralde H, Havlin S, Stanley HE. Phys Rev B. 1994; 50:15316.
21. Barabási, A-L.; Stanley, HE. Fractal Concepts in Surface Growth. Cambridge Univ. Press; Cambridge, UK: 1995.
22. Ratsch C, Zangwill A, Smilauer P, Vvedensky DD. Phys Rev Lett. 1994; 72:3194. [PubMed: 10056131]
23. Ghaisas SV, Sarma SD. Phys Rev B. 1992; 46:7308.
24. Barrat A, Silberzan P, Bourdieu L, Chatenay D. Europhys Lett. 1992; 20:633.
25. Bierbaum K, Grunze M. Langmuir. 1995; 11:2143.
26. Tripp CP, Hair ML. Langmuir. 1992; 8:1120.
27. Tripp CP, Hair ML. Langmuir. 1995; 11:149.
28. Carson GA, Granick S. J Mater Res. 1990; 5:1745.
29. Brzoska JB, Azouz IB, Rondelez F. Langmuir. 1994; 10:4367.
30. Brzoska JB, Shahidzadeh N, Rondelez F. Nature. 1992; 360:719.
31. Parikh AN, Allara DL, Azouz IB, Rondelez F. J Phys Chem. 1994; 98:7577.
32. Israelachvili, J. Intermolecular and Surface Forces. Academic Press Ltd; San Diego: 1992.
33. Stroscio JA, Pierce DT. Phys Rev B. 1994; 49:8522.
34. Michely T, Hohage M, Bott M, Comsa G. Phys Rev Lett. 1993; 70:3943. [PubMed: 10054005]
35. Cohen SR, Naaman R, Sagiv J. J Phys Chem. 1986; 90:3054.
36. Whitesidcs GM, Mathias JP, Seto CT. Science. 1991; 254:1312. [PubMed: 1962191]

37. Pashley RM. J Colloid Interface Sci. 1981; 83:531.

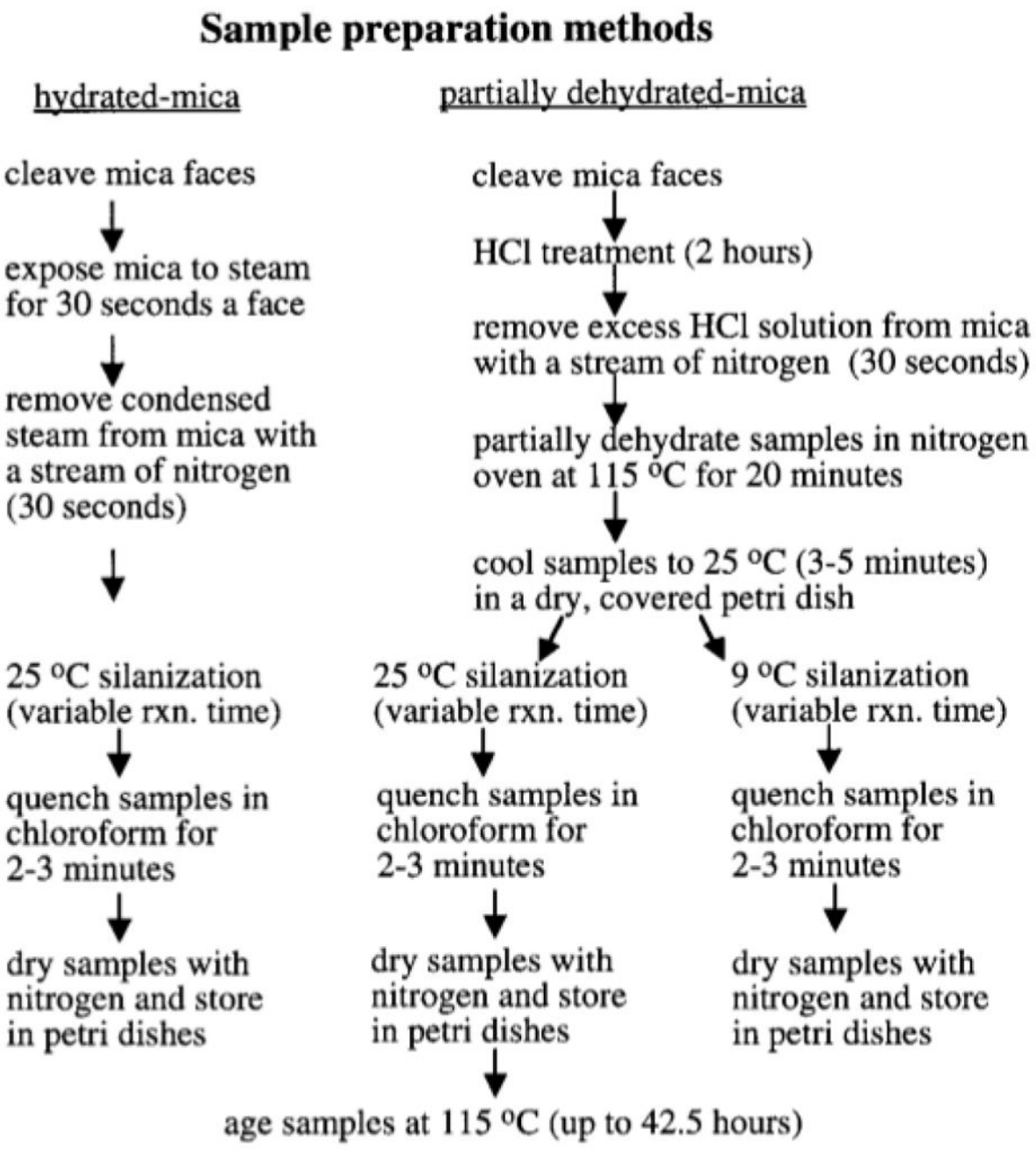

FIG. 1.
Pretreatment and silanization methods for mica substrates.

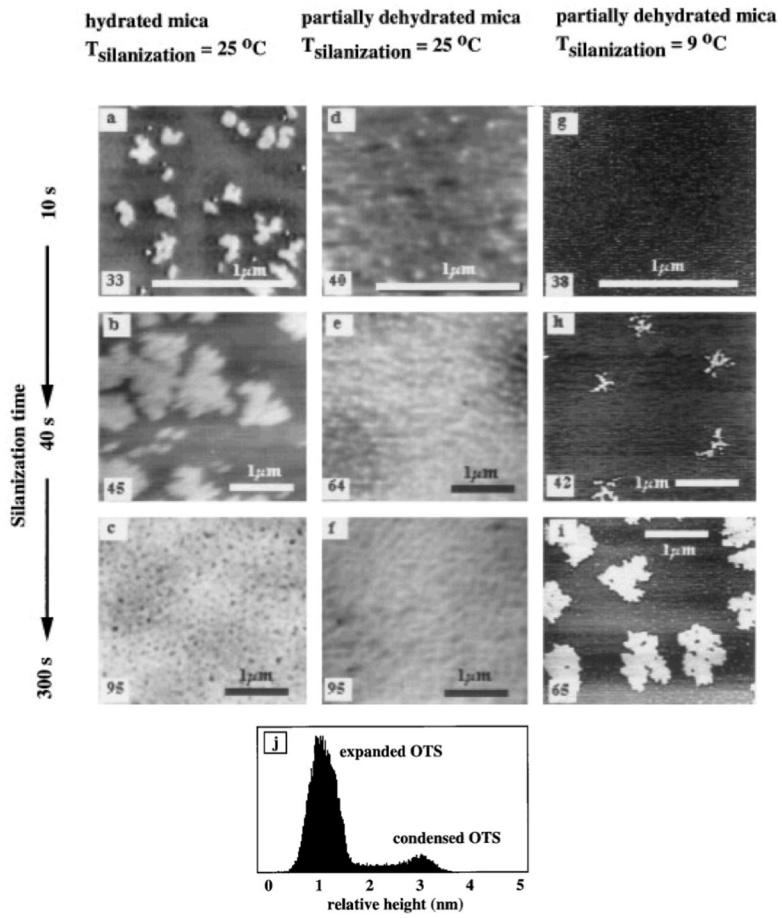

FIG. 2.

The effects of silanization temperature and hydration state versus silanization time on the formation of OTS monolayers. The numbers in the bottom left corners of each image represent the water contact angle for that sample, (a, b, c) Three different hydrated mica samples silanized for 10, 40, and 300 s, respectively, (d, c, f) Three different partially dehydrated samples silanized for 10, 40, and 300 s, respectively, (g, h, i) Three different partially dehydrated samples silanized for 10, 40, and 300 s at a silanization temperature of 9°C. Note: The gray scales are slightly different for each panel and cannot be directly compared. (j) A histogram of (a) clearly indicates the presence of both condensed and expanded OTS phases.

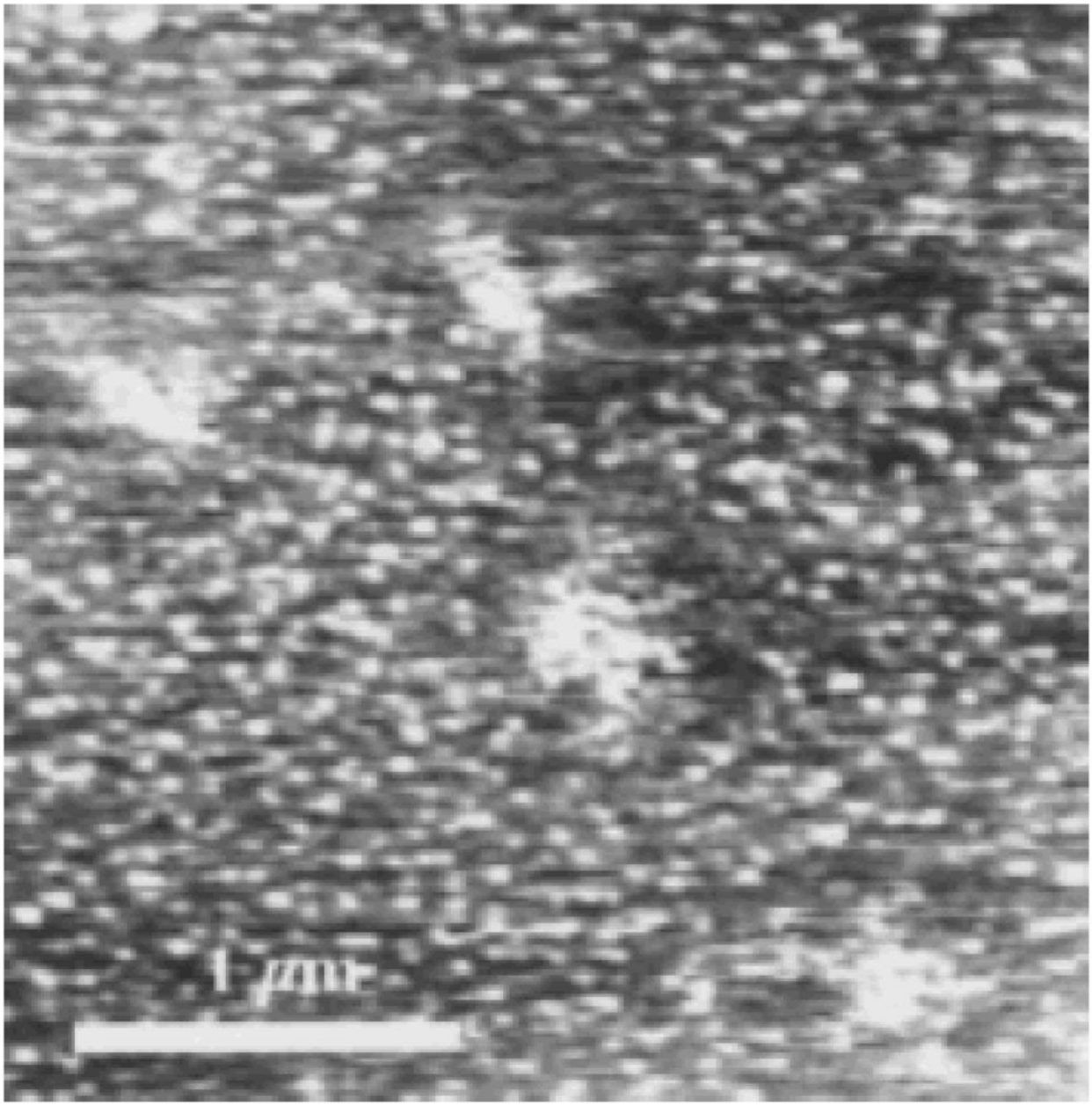

FIG. 3.

A partially dehydrated mica sample silanized at 9°C for 40 s. The clusters which have aggregated to form larger islands have left depleted areas around these islands.

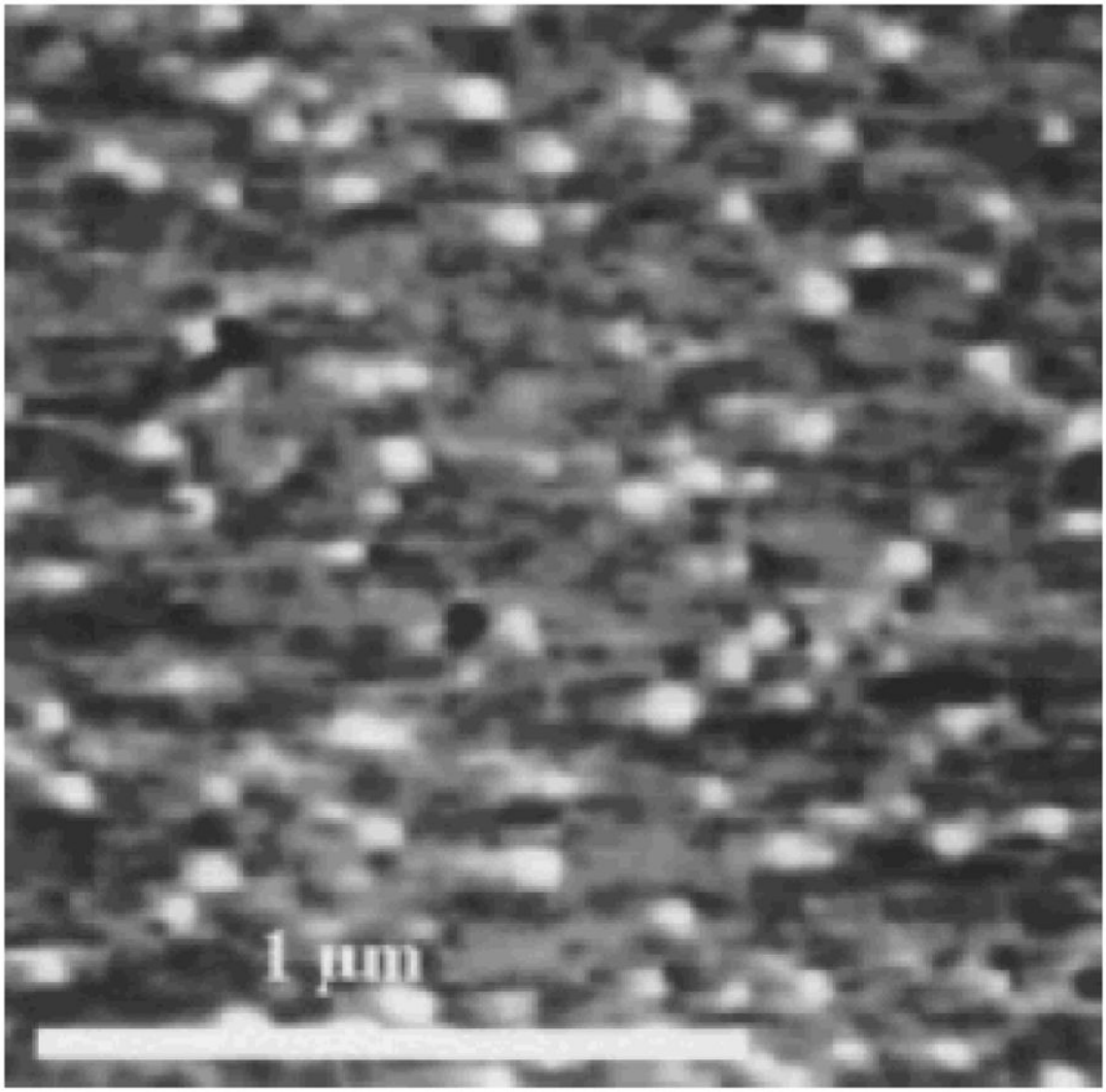

FIG. 4.

The effects of 42.5 h of annealing at 115°C on the sample shown in Fig. 2d (partially dehydrated mica silanized at 25°C for 10 s). Note the presence of many more clusters in this image compared with Fig. 2d. The sample contact angle has not changed during annealing.

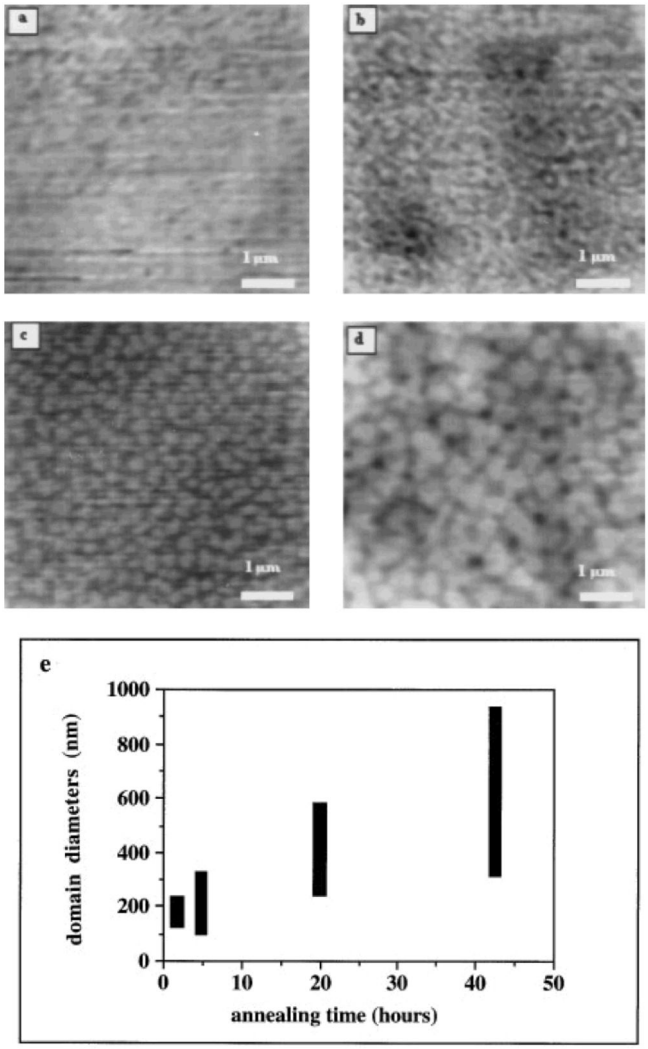

FIG. 5.

Annealing induced OTS domain aggregation on the sample shown in Fig. 2f. The 115°C annealing process was interrupted at various times to allow the sample to be imaged with the AFM. After AFM analysis, the sample was immediately returned to the nitrogen oven for additional annealing. The sample after (a) 1.5 h of annealing; (b) 4.75 h; (c) 19.75 h; (d) 42.5 h. The average diameters of the condensed domains steadily increase with annealing due to enhanced surface diffusion and aggregation of the adsorbed OTS (shown in (e)).